Cascades of reversible homoclinic orbits to a saddle-focus equilibrium

Jörg Härterich

Freie Universität Berlin, Arnimallee 2-6, D-14195 Berlin

Abstract

In a reversible system, we consider a homoclinic orbit being bi-asymptotic to a saddle-focus equilibrium. As was proved by Devaney, there exists a one-parameter family of periodic orbits accumulating onto this homoclinic orbit.

In the present paper, we show that for any $n \geq 2$ there exist infinitely many n-homoclinic orbits in a neighborhood of the primary homoclinic orbit . Each of them is accompanied by one or more families of periodic orbits. Moreover, we indicate how these families of periodic orbits correspond to branches of subharmonic periodic orbits.

1 Introduction

Homoclinic orbits are well-known to have a great influence on the dynamics in a neighborhood. In systems with a parameter, homoclinic orbits are typically destroyed under small perturbations. However, in many cases one can find periodic orbits, n-homoclinic orbits or shift dynamics at parameter values that are close to the value where the primary homoclinic orbit exists. The situation is different in reversible or Hamiltonian systems, since homoclinic orbits generically persist under small perturbations that respect the reversible or Hamiltonian structure. It is then often possible to find many other homoclinic or periodic orbits not only for slightly different, but for the same parameter value as the primary homoclinic orbit. Devaney [Dev77] has shown that homoclinic orbits are accompanied by a one-parameter-family of periodic orbits. For periodic orbits in reversible systems, Vanderbauwhede [Van90] found branches of subharmonic periodic orbits at the same parameter value if one Floquet multiplier of a periodic orbit equals a root of unity. The main focus in this paper is on homoclinic and periodic orbits that make several revolutions inside a tubular neighborhood of the primary homoclinic orbit.

Our viewpoint is a geometrical one: We describe the image of certain sets

under a Poincaré-map and their intersections. This enables us to find many homoclinic and periodic orbits. Moreover, we can identify some families of periodic orbits accompanying the homoclinic orbits as branches of subharmonic periodic orbits.

The work presented in this paper is an extension of [Här93] and is closely related to a paper of Champneys [Cha94]. Although in both papers similar results are proved, the emphasis is different. While Champneys concentrates mainly on 2- and 3-homoclinic solutions without generalizing to n-homoclinics, we try to describe as completely as possible all reversible homoclinic and periodic orbits in a neighborhood of the primary homoclinic. In contrast, Champneys also presents an example and numerically locates some of the theoretically predicted homoclinic orbits.

The paper is organized as follows. After some preliminaries in section 2, we give the basic assumptions and results in section 3. A linearization result is used in section 4 to simplify the Poincaré-map. The geometrical objects that will prove useful later are introduced in section 5. Section 6 contains the proofs. and the paper concludes with a short discussion.

2 Reversible dynamical systems

Consider an ordinary differential equation

$$\dot{x} = f(x) \quad , \qquad x \in \mathbb{R}^{2m} \quad , \quad f \in C^k \quad (k \geq 2). \tag{1}$$

Definition 1 *Equation (1) is called* reversible*, if there is a linear involution* $R : \mathbb{R}^{2m} \to \mathbb{R}^{2m}$ *with* $R^2 = id$ *and* $dim(Fix(R)) = m$ *such that the reversibility condition*

$$f(Rx) = -Rf(x) \qquad \forall x \in \mathbb{R}^{2m} \tag{2}$$

holds.

One of the most useful properties of reversible systems is the fact that together with $x(t)$ also $Rx(-t)$ is a solution of equation (1).
For the flow Φ_t generated by (1) this fact can be expressed by the relation

$$\Phi_t = R\,\Phi_{-t}\,R. \tag{3}$$

Definition 2 *An orbit* γ *is called* reversible *if* $R(\gamma) = \gamma$.

Since reversibility does not affect orbits that stay away from the plane $Fix(R)$, we will focus our attention almost exclusively on reversible orbits.

The following classification of reversible orbits is taken from [VF92].

Proposition 3 [Vanderbauwhede & Fiedler] *An orbit γ of a reversible dynamical system is reversible iff $\gamma \cap Fix(R) \neq \emptyset$. Then exactly one of the following three situations occurs:*
(i) $\gamma \subseteq Fix(R)$ and γ is a reversible equilibrium.
(ii) $\gamma \not\subseteq Fix(R), \gamma \cap Fix(R)$ consists of a single point and γ is not a closed trajectory.
(iii) $\gamma \cap Fix(R)$ consists of precisely two points and γ is a reversible periodic orbit.

Reversible homoclinic orbits are contained in the second class and have a unique symmetric point where they intersect the plane $Fix(R)$. Note that the equilibrium to which a reversible homoclinic orbit converges has to be a reversible equilibrium.
Reversibility also affects the linearization at a reversible equilibrium $x_0 \in Fix(R)$. By simple calculations one can verify the following two properties:

Proposition 4 *The linearization $A := Df(x_0)$ satisfies:*
(i) $AR = -RA$
(ii) λ is an eigenvalue of $A \Leftrightarrow -\lambda$ is an eigenvalue of A.

Hence, if one of the eigenvalues is a complex number $\alpha+\omega i$ with $\alpha, \omega \neq 0$, then automatically the quadruple $\pm\alpha \pm \omega i$ is contained in the spectrum of A. In $\mathbb{R}^4$, an equilibrium with such a quadruple of eigenvalues is called a *saddle-focus equilibrium*.

3 The Setting and main results

In the rest of the paper we restrict ourselves to equations in $\mathbb{R}^4$. We consider therefore the differential equation (1) with $m = 2$ and make the following five assumptions:

(A1) the reversibility condition $f(Rx) = -Rf(x)$ holds
(A2) $f(0) = 0$, i.e. the origin is a reversible equilibrium
(A3) the spectrum of the Jacobian $Df(0)$ consist of the four complex eigenvalues $\pm\alpha \pm i\omega \quad (\alpha, \omega > 0)$
(A4) there exists a reversible homoclinic orbit γ satisfying

$$\lim_{t \to \pm\infty} \gamma(t) = 0 \tag{4}$$

(A5) γ is *nondegenerate*, i.e. the tangent spaces of the stable and unstable manifold satisfy

$$\dim(T_{\gamma(t)}W^{\mathrm{s}}(0) \cap T_{\gamma(t)}W^{\mathrm{u}}(0)) = 1.$$

Sometimes it is useful to replace assumption **(A5)** by the weaker assumption that γ is a *elementary* homoclinic orbit:

(A5') Let $q := \gamma \cap Fix(R)$. Then the stable manifold $W^{\mathrm{s}}(0)$ and the plane $Fix(R)$ do intersect each other transversally in q. Moreover, γ does not belong to a one-parameter-family of homoclinic orbits.

The restriction to $\mathbb{R}^4$ is not too strict. A reduction from a higher-dimensional problem to this four-dimensional situation can in many cases be achieved by a center-manifold reduction near the homoclinic orbit γ, see [San95]. **(A3)** states a resonance between eigenvalues which prevents an application of Shil'nikovs results [Shi67] on saddle-focus homoclinic orbits. Assumption **(A5)** and **(A5')** both imply that the homoclinic orbit γ is structurally stable (in the class of reversible dynamical systems).

Our main interest will be in orbits that make several excursions along the homoclinic orbit γ.

Definition 5 *An orbit is called* k-homoclinic, *if it is entirely contained in a tubular neighborhood of the homoclinic orbit* γ *and if it hits a transverse section to* γ *exactly* k *times.*

Analogously, an orbit is called k-periodic *if it is contained in a tubular neighborhood of* γ *and if it hits a transverse section to* γ *exactly* k *times before closing up at the* $(k+1)$*-th time.*

We do not assume k to be minimal, a k-periodic orbit therefore also is nk-periodic for any $n \in \mathbb{N}$.

We have the following main theorem.

Theorem 6 *Assume* **(A1)**-**(A5)**. *Then for any* $n \geq 2$ *there exist infinitely many* n*-homoclinic orbits in a tubular neighborhood of* γ. *Moreover, to each* n*-homoclinic orbit there is a one-parameter family of reversible* n*-periodic orbits accumulating onto the* n*-homoclinic orbit.*

If **(A5)** is replaced by **(A5')** the following weaker version holds:

Theorem 7 *Assume* **(A1)**-**(A4)** *and* **(A5')**. *Then there exist infinitely many 2-homoclinic and 3-homoclinic orbits in a tubular neighborhood of* γ. *Either all of them are degenerate or there is a nondegenerate homoclinic orbit for which theorem 6 applies.*

4 The Poincaré-map

The proof of theorem 6 uses a Poincaré-map along the homoclinic orbit γ. This Poincaré-map is divided into a local part (near 0) and a global diffeomorphism along γ.

4.1 The local part

For the local part a C^1-linearization of the flow near the origin will prove useful.

Lemma 8 [linearization, Belitskii(1973)] *If the eigenvalues of $Df(0)$ satisfy assumption* **(A3)**, *the flow can be C^1-linearized locally near* 0.

Proof. The proof is based on a theorem of Belitskii [Bel73] for diffeomorphisms. He shows that for any diffeomorphism $\Phi_1 \in C^2(\mathbb{R}^n)$ with $\Phi_1(0) = 0$ there is a neighborhood $\mathbf{U}$ of 0 and a C^1-diffeomorphism $h_0 : \mathbf{U} \to \mathbf{U}$, such that Φ_1 is locally conjugate to its linear part, i.e.

$$h_0 \circ \Phi_1 \circ h_0^{-1} = D\Phi_1(0) \tag{5}$$

in $\mathbf{U}$, if for all eigenvalues $\lambda_i, \lambda_j, \lambda_k$ of $D\Phi_1(0)$ the condition

$$|\lambda_i| \neq |\lambda_j| \cdot |\lambda_k| \qquad (\forall\, |\lambda_j| \leq 1 \leq |\lambda_k|) \tag{6}$$

holds.
The linearization of the time-1-map Φ_1 of (1) at 0 has eigenvalues $e^{\pm\alpha \pm i\omega}$, and it is easily seen that for $\alpha \neq 0$ the condition (6) holds. Using a standard argument (see e. g. [Har82]) one can construct a linearization for the flow Φ_t from the linearization of the time-1-map Φ_1.

□

Without restriction, we assume now that the reversibility condition **(A1)** holds for the matrix

$$R = \begin{pmatrix} 0 & 0 & 1 & 0 \\ 0 & 0 & 0 & 1 \\ 1 & 0 & 0 & 0 \\ 0 & 1 & 0 & 0 \end{pmatrix}$$

and that the linear flow in a small neighborhood $\mathbf{U}$ of 0 is generated by the differential equation

$$\dot{x} = \begin{pmatrix} \alpha & -\omega & 0 & 0 \\ \omega & \alpha & 0 & 0 \\ 0 & 0 & -\alpha & \omega \\ 0 & 0 & -\omega & -\alpha \end{pmatrix} x \ .$$

For the construction of the Poincaré-map near the homoclinic orbit γ it is convenient to choose polar coordinates in $\mathbf{U}$. To this end, set

$$\begin{aligned} x_1 &= \varrho_{\mathrm{u}} \cos\varphi_{\mathrm{u}} \qquad , \qquad x_2 = \varrho_{\mathrm{u}} \sin\varphi_{\mathrm{u}}, \\ x_3 &= \varrho_{\mathrm{s}} \cos\varphi_{\mathrm{s}} \qquad , \qquad x_4 = \varrho_{\mathrm{s}} \sin\varphi_{\mathrm{s}}, \end{aligned}$$

with indices u, s indicating the unstable and stable directions, respectively. The local stable and unstable manifolds are then

$$W^{\mathrm{s}}_{\mathrm{loc}}(0) = \{\, \varrho_{\mathrm{u}} = 0 \,\} \qquad , \qquad W^{\mathrm{u}}_{\mathrm{loc}}(0) = \{\, \varrho_{\mathrm{s}} = 0 \,\}$$

and the plane $Fix(R)$ is given as

$$Fix(R) = \{\ \varrho_{\mathrm{s}} = \varrho_{\mathrm{u}}\ ,\ \varphi_{\mathrm{s}} = \varphi_{\mathrm{u}}\}.$$

In the new coordinates, the differential equation reads

$$\begin{aligned} \dot{\varrho_{\mathrm{u}}} &= \alpha\varrho_{\mathrm{u}} \qquad , \qquad \dot{\varphi_{\mathrm{u}}} = \omega \\ \dot{\varrho_{\mathrm{s}}} &= -\alpha\varrho_{\mathrm{s}} \qquad , \qquad \dot{\varphi_{\mathrm{s}}} = -\omega. \end{aligned} \tag{7}$$

The explicit solution of this equation is

$$\begin{aligned} \varrho_{\mathrm{u}}(t) &= \varrho_{\mathrm{u}}(0) \cdot e^{\alpha t} \qquad , \qquad \varphi_{\mathrm{u}}(t) = \varphi_{\mathrm{u}}(0) + \omega t \\ \varrho_{\mathrm{s}}(t) &= \varrho_{\mathrm{s}}(0) \cdot e^{-\alpha t} \qquad , \qquad \varphi_{\mathrm{s}}(t) = \varphi_{\mathrm{s}}(0) - \omega t. \end{aligned} \tag{8}$$

In view of our subsequent analysis, we divide the local part of the Poincaré-map in two mappings that are related by reversibility. To this end, we define transverse sections Σ^{u}, Σ^0 and Σ^{s} as

$$\Sigma^{\mathrm{u}} := \{\, \varrho_{\mathrm{u}} = r,\ \varrho_{\mathrm{s}} \le r \,\},\ \Sigma^{\mathrm{s}} := R(\Sigma^{\mathrm{u}}) \text{ and } \Sigma^0 := \{\, \varrho_{\mathrm{u}} = \varrho_{\mathrm{s}} \le r\}.$$

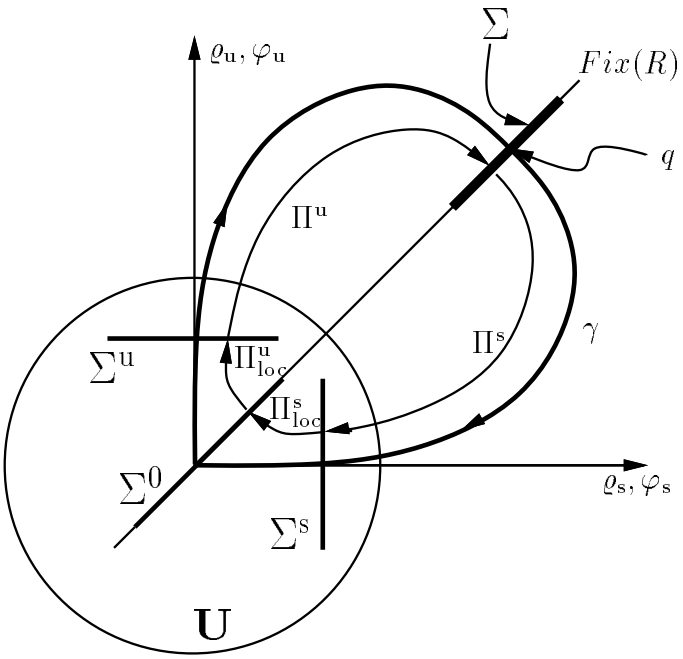

Figure 1: The Poincaré-map along γ

Here $r > 0$ is chosen sufficiently small such that trajectories from Σ^s to Σ^u lie entirely in $\mathbf{U}$ where the vector field is linear, compare figure 1. The sections Σ^s and Σ^u are solid tori with $W^s_{loc}(0) \cap \Sigma^s$ and $W^u_{loc}(0) \cap \Sigma^u$ being their centre circles, see figure 2. The section Σ^0 in between is R-invariant. Denote with $q^s := \Sigma^s \cap \gamma$ and $q^u := \Sigma^u \cap \gamma$ the points where the homoclinic orbit γ crosses the sections Σ^s and Σ^u. The (linear) flow now defines a local Poincaré-map

$$\Pi^s_{loc} : \Sigma^s \setminus W^s_{loc}(0) \to \Sigma^0 \setminus \{0\}$$

that can be written down explicitly. Reversibility also yields another flow-induced local Poincaré-map

$$\Pi^u_{loc} = R \circ (\Pi^s_{loc})^{-1} \circ R : \Sigma^0 \setminus \{0\} \to \Sigma^s \setminus W^s_{loc}(0)$$

Putting these two mappings together, we receive the local Poincarè-map $\Pi_{loc} := \Pi^u_{loc} \circ \Pi^s_{loc}$. We will describe Π_{loc} in the form

$$\Pi_{loc} : (\varrho_u^{in}, \varphi_u^{in}, \varphi_s^{in}) \to (\varphi_u^{out}, \varrho_s^{out}, \varphi_s^{out}). \tag{9}$$

The time t_f a trajectory spends between $\Sigma^s \setminus W^s_{loc}(0)$ and Σ^u satisfies the equation

$$\varrho_u(t_f) = r$$

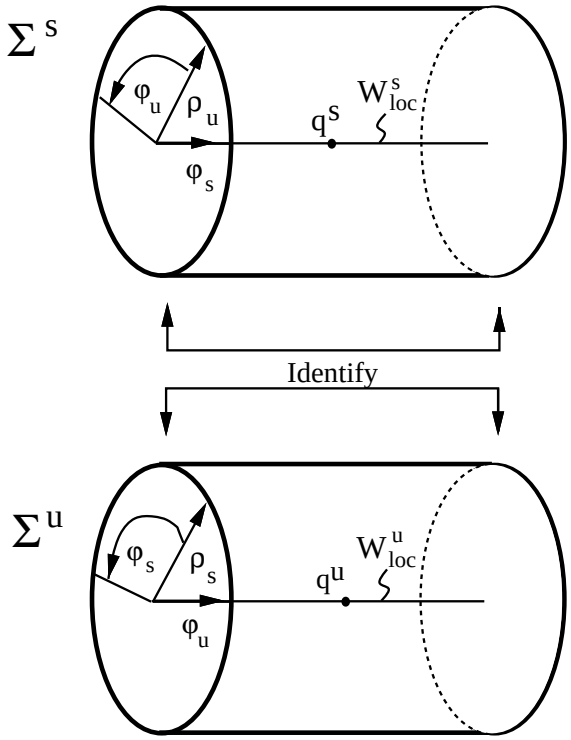

Figure 2: The transverse sections Σ^{s} and Σ^{u}

which yields

$$t_f = \alpha^{-1} \log \frac{r}{\varrho_{\mathrm{u}}^{\mathrm{in}}}. \tag{10}$$

Substituting this into (8) gives

$$\begin{aligned} \varrho_{\mathrm{s}}^{\mathrm{out}} &= \varrho_{\mathrm{u}}^{\mathrm{in}} \\ \varphi_{\mathrm{s}}^{\mathrm{out}} &= \varphi_{\mathrm{s}}^{\mathrm{in}} - \tfrac{\omega}{\alpha} \log \tfrac{r}{\varrho_{\mathrm{u}}^{\mathrm{in}}} \\ \varphi_{\mathrm{u}}^{\mathrm{out}} &= \varphi_{\mathrm{u}}^{\mathrm{in}} + \tfrac{\omega}{\alpha} \log \tfrac{r}{\varrho_{\mathrm{u}}^{\mathrm{in}}} \end{aligned} \tag{11}$$

as an expression for the local Poincaré map Π_{loc}. Similar equations can be derived for the maps $\Pi_{\mathrm{loc}}^{\mathrm{s}}$ and $\Pi_{\mathrm{loc}}^{\mathrm{u}}$.

4.2 The global map

In a similar way, we can make use of the reversibility in the construction of the global Poincaré-map by taking a R-invariant cross-section Σ containing the point $q := \gamma \cap Fix(R)$. A local diffeomorphism Π^{s} between Σ and Σ^{s} is

induced by the flow along γ. This diffeomorphism Π^s maps a neighborhood of q in Σ onto a neighborhood of q^s in Σ^s. Analogously, $\Pi^u : \Sigma^u \to \Sigma$ is induced by the flow along γ. By reversibility $\Pi^u = R \circ (\Pi^s)^{-1} \circ R$ and the mapping $\Pi : \Sigma \to \Sigma$ with

$$\Pi = \Pi^u \circ \Pi_{loc} \circ \Pi^s \tag{12}$$

is a Poincaré-map following the homoclinic orbit γ once. Note that this map is a reversible map, i.e. $R \circ \Pi \circ R = \Pi^{-1}$. For later use, we also define two Poincaré-maps that follow only one half of γ as

$$\Pi^s_{1/2} := \Pi^s_{loc} \circ \Pi^s \text{ and } \Pi^u_{1/2} := \Pi^u \circ \Pi^u_{loc}.$$

Those Poincaré-maps enable us to find all reversible periodic orbits near γ. Since orbits lying in a tubular neighborhood of γ can intersect $Fix(R)$ only in Σ or in Σ^0, there are three different possibilities how the two symmetric points of a reversible periodic orbit can lie in Σ or in Σ^0. These three cases are distinguished in the following lemma.

Lemma 9

(i) If $x \in Fix(R) \cap \Pi^n(Fix(R))$, then $x \in \Sigma$ is a fixed point of Π^{2n}. The associated trajectory of (1) through x is reversible and $2n-$periodic.

(ii) If $x \in Fix(R) \cap (\Pi^s_{1/2} \circ \Pi^{n-1} \circ \Pi^u_{1/2})(Fix(R))$, then $x \in \Sigma^0$ is a fixed point of Π^{2n}. The associated trajectory of (1) through x is reversible and $2n-$periodic.

(iii) If $x \in Fix(R) \cap (\Pi^n \circ \Pi^u_{1/2})(Fix(R))$, then $x \in \Sigma$ is a fixed point of Π^{2n+1}. The associated trajectory of (1) through x is reversible and $(2n+1)$-periodic.

Proof. We will only show (i), since (ii) and (iii) can be proved analogously. In case (i) $x = \Pi^n(y)$ for some $y \in Fix(R) \cap \Sigma$.
Hence

$$\begin{aligned} & \Pi^{-n}(y) = R\,\Pi^n(Ry) = R\,\Pi^n(y) = Rx = x \\ \Rightarrow \quad & \Pi^{2n}(x) = x \end{aligned}$$

and x lies on a $2n$-periodic orbit.

□

In a similar way reversibility provides us with a tool to detect reversible homoclinic orbits which pass through a tubular neighborhood of γ several times before eventually entering a small neighborhood of the equilibrium.

To this end, define $W^{\mathrm{s}}_q := (\Pi^{\mathrm{s}})^{-1}(W^{\mathrm{s}}_{\mathrm{loc}}(0) \cap \Sigma^{\mathrm{s}})$ as the component of $W^{\mathrm{s}}(0) \cap \Sigma$ passing through q. Similarly, $W^{\mathrm{u}}_q := \Pi^{\mathrm{u}}(W^{\mathrm{u}}_{\mathrm{loc}}(0) \cap \Sigma^{\mathrm{u}}) = R(W^{\mathrm{s}}_q)$ is the component of $W^{\mathrm{u}}(0)$ in Σ containing the point q.

Hence, each orbit starting in W^{s}_q tends directly to 0, i.e. it does not leave the neighborhood $\mathbf{U}$ of 0 again once it has entered $\mathbf{U}$.
We have to distinguish two cases: Homoclinic orbits that follow γ an odd number of times have their symmetric point in Σ, while $2n$-homoclinic orbits intersect $Fix(R)$ in Σ^0.

Lemma 10

(i) If $x \in W^{\mathrm{s}}_q \cap \Pi^n(Fix(R))$ then the associated orbit is a reversible $(2n+1)$-homoclinic orbit.
(ii) If $x \in W^{\mathrm{s}}_q \cap (\Pi^n \circ \Pi^{\mathrm{u}}_{1/2})(Fix(R))$ then the associated orbit is a reversible $(2n+2)$-homoclinic orbit.

Proof. The proof consists of simple counting arguments:
(i) We have $\Pi^{-n}(x) \in Fix(R)$, hence $\Pi^{-2n}(x) \in W^{\mathrm{u}}_q$, the whole orbit therefore follows the orbit γ exactly $2n$ times from Σ back to Σ and another two "half" times from Σ to 0.
(ii) Here the orbit through x follows γ exactly $n + 1/2$ times until it hits W^{s}_q and settles down at 0 after another half revolution. Completing the orbit backward by reversibility yields a $(2n+2)$-homoclinic orbit.

□

5 Spirals & Scrolls

To describe the effect of the Poincaré-map Π on $Fix(R)$ we introduce the notion of spirals and scrolls.

Definition 11 *A C^1-curve κ on a two-dimensional manifold $\mathcal{M}$ is called* (logarithmic) spiral *on $\mathcal{M}$, if there is a $\beta \neq 0$, a neighborhood $W \subseteq \mathbb{R}^2$ of 0 and a local diffeomorphism $\Psi : \mathcal{M} \supseteq V \to W$, such that the image $\Psi(\kappa \cap V)$ is the part of a logarithmic spiral S_β lying in W. This reference spiral S_β is given in planar polar coordinates by the parametrization*

$$r(\tau) = e^{\beta\tau}$$
$$\varphi(\tau) = \tau, \qquad \tau \in \mathbb{R}$$

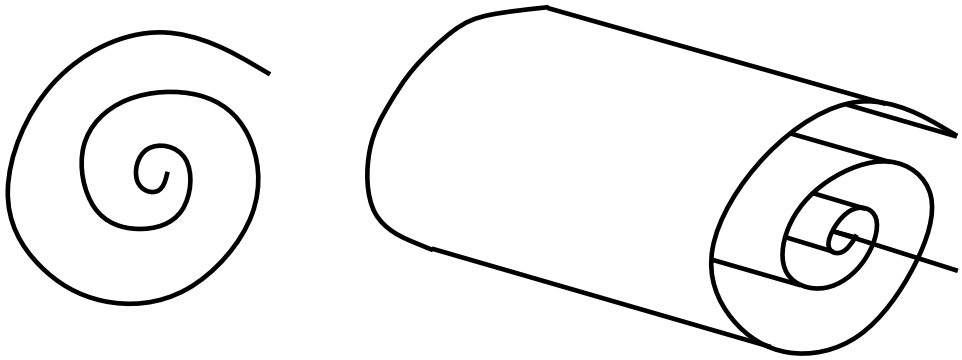

Figure 3: A logarithmic spiral and a logarithmic scroll

$\Psi^{-1}(0)$ *is called the* base point *of the spiral.*

An imbedded two-dimensional manifold $\mathcal{N} \subseteq \mathbb{R}^3$ *is called* (logarithmic) scroll, *if there is a reference spiral* S_β *as above, neighborhoods* $V_0 \subseteq \mathbb{R}^3$, $W_0 \subseteq \mathbb{R}^2$ *of* 0 *and a diffeomorphism* $\Psi_0 : V_0 \to [\,0,1\,] \times W_0$ *such that the image* $\Psi_0(\mathcal{N} \cap V_0)$ *is* $[\,0,1\,] \times (S_\beta \cap W_0)$.
The pre-image $\Psi_0^{-1}([\,0,1\,] \times \{0\})$ *is called the* basis *of the scroll.*

Remark 12

(i) The terms spiral & scroll are related to the 0- *resp.* 1*-spirals introduced by Devaney in [Dev77].*
(ii) A C^1*-diffeomorphism* $\hat{\Psi} : \mathcal{N} \to \hat{\mathcal{N}}$ *maps a spiral on a manifold* $\mathcal{N}$ *into a spiral on the manifold* $\hat{\mathcal{N}}$*.*
(iii) If $\Phi : \mathbb{R}^3 \to \mathbb{R}^3$ *is a* C^1*-diffeomorphism, then the image of a scroll under* Φ *is a scroll again.*

Since spirals and scrolls will appear as images of certain sets under iterates of the Poincaré-map it will prove useful to know how their intersection with curves and planes looks like. In particular, curves intersecting the basis of a scroll always intersect the scroll itself in infinitely many points.

Lemma 13

(i) A C^1*-curve* κ *on a manifold* $\mathcal{M}$ *passing through the base point* p *of a spiral* $\mathcal{S}$ *on* $\mathcal{M}$*, intersects this spiral in infinitely many points, that accumulate onto* p*.*
(ii) A C^1*-curve* κ *in* $\mathbb{R}^3$*, intersecting the basis of a logarithmic scroll in* p *in such a way that* κ *and the basis are not tangential at* p *intersects the scroll in infinitely many points* $p_1, p_2, p_3, \ldots$ *accumulating onto* p*. Furthermore, there is an* i_0*, such that for all* $i \geq i_0$ *the intersection of* κ *and the scroll is transverse.*

(ii') *A C^1-curve κ in $\mathbb{R}^3$, that is tangential to the basis of a logarithmic scroll in p but does not coincide with the basis in a neighborhood of p, intersects the scroll in infinitely many points $p_1, p_2, p_3, \ldots$ accumulating onto p.*

(iii) *If a plane $\mathcal{E}$ intersects the basis of a logarithmic scroll $\mathcal{R}$ transversally in p, then $\mathcal{E} \cap \mathcal{R}$ locally (i.e. near p) is a spiral in $\mathcal{E}$ with base point p.*

Proof. (i) There is a diffeomorphism Ψ mapping a neighborhood V of p on $\mathcal{M}$ into $\mathbb{R}^2$ such that the image $\Psi(\kappa \cap V)$ is a C^1-curve in $\mathbb{R}^2$ through 0. This curve intersects the spiral $S_\beta = \Psi(\mathcal{S} \cap V)$ in infinitely many points accumulating onto 0. The pre-image of those points on $\mathcal{M}$ are exactly the points of intersection between κ and $\mathcal{S}$.
(ii) and (ii') are proved similarly to (i) by transformation to a "standard scroll" $[0,1] \times S_\beta$.
(iii) Let Ψ_0, V_0, W_0 and the logarithmic spiral S_β be chosen as in definition 11, such that $\Psi_0(\mathcal{R} \cap V_0) = [0,1] \times (S_\beta \cap W_0)$ and let W_0 be sufficiently small such that the C^1-manifold $\Psi_0(\mathcal{E}) \cap ([0,1] \times W_0)$ which is transversal to $[0,1] \times \{0\}$ can be written as a graph over $\{0\} \times W_0$.
The projection $\pi : \Psi_0(\mathcal{E}) \cap ([0,1] \times W_0) \to W_0$ is then a diffeomorphism. Therefore, $\pi \circ \Psi_0$ is also a diffeomorphism mapping $\mathcal{R} \cap \mathcal{E}$ locally onto the spiral S_β and p to the base point of that spiral.
Thus, $\mathcal{R} \cap \mathcal{E}$ itself is a spiral in $\mathcal{E}$ with base point p.

□

The main connection between the geometrical concept of spirals & scrolls and reversible homoclinic orbits is given by the following lemma. Essentially it says that a part of any surface which intersects the curve W^{s}_q transversally in Σ will be mapped to a logarithmic scroll by the Poincaré-map Π.

Lemma 14 *Let $\mathcal{F}$ be a two-dimensional C^1-manifold in Σ, intersecting W^{s}_q transversally in p. Then for any closed interval $I \subset W^{\mathrm{u}}_{\mathrm{loc}}(0) \cap \Sigma^{\mathrm{u}}$ there is a subset $\mathcal{F}_{\mathrm{I}}$ of $\mathcal{F}$, such that $(\Pi_{\mathrm{loc}} \circ \Pi^{\mathrm{s}})(\mathcal{F}_I)$ is a logarithmic scroll in Σ^{u} with basis I.*
The point p lies on the boundary of $\mathcal{F}_{\mathrm{I}}$ (see figure 4).

Proof. Since Π^{s} is a local diffeomorphism mapping a neighborhood of p in Σ to Σ^{s} it suffices to show: If a two-dimensional C^1-manifold $\mathcal{M} = \Pi^{\mathrm{s}}(\mathcal{F})$ in Σ^{s} intersects $W^{\mathrm{s}}_{\mathrm{loc}}(0)$ transversally in a point $m = \Pi^{\mathrm{s}}(p)$ then there exists a subset $\mathcal{M}_I$ of $\mathcal{M}$ that is mapped to a logarithmic scroll with basis I by Π_{loc}.
To prove this claim, we first restrict the ϱ_{u}-coordinate in Σ^{s} to $\varrho_{\mathrm{u}} \le \tilde{r}$ with appropriately chosen $0 < \tilde{r} \le r$. Thereby, we get a neighborhood $\mathcal{M}_0$ of m in $\mathcal{M}$, such that $\mathcal{M}_0$ can be written as the graph of a C^1-function g:

$$\mathcal{M}_0 = \{\, (\varphi_{\mathrm{s}}, \varphi_{\mathrm{u}}, \varrho_{\mathrm{u}}) \in \Sigma^{\mathrm{s}} \;;\; \varphi_{\mathrm{s}} = g(\varrho_{\mathrm{u}} \cos(\varphi_{\mathrm{u}}), \varrho_{\mathrm{u}} \sin(\varphi_{\mathrm{u}})) \;,\; \varrho_{\mathrm{u}} \le \tilde{r} \,\} \quad (13)$$

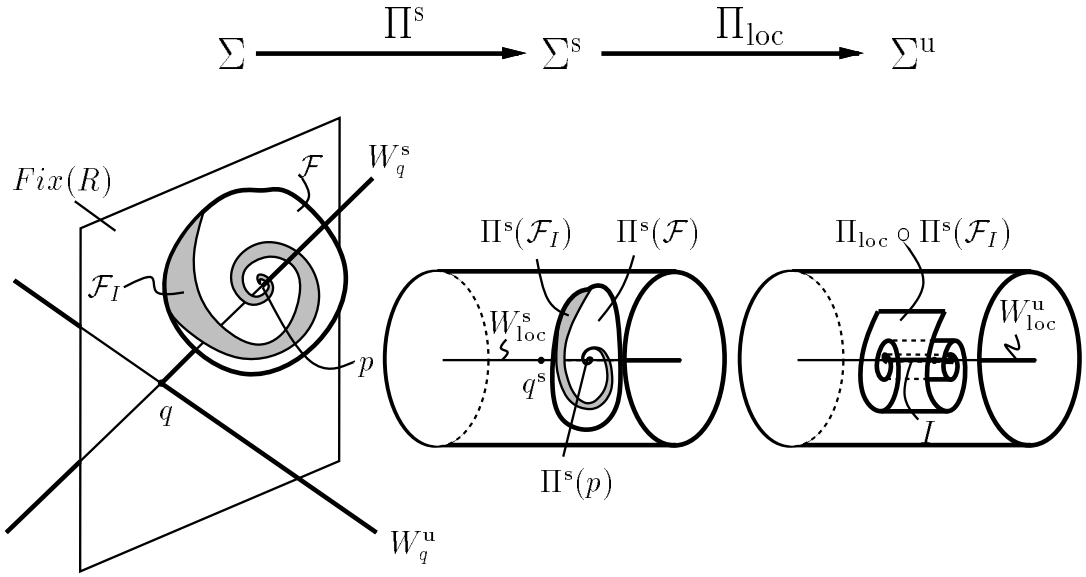

Figure 4: The effect of the local Poincaré-map on a surface

Define then $\mathcal{M}_I \subseteq \mathcal{M}_0$ to be those points of $\mathcal{M}_0$ that are mapped by Π_{loc} onto points with φ_{u}-coordinate in I. Hence, by (11)

$$\mathcal{M}_I = \{\ (\varphi_{\mathrm{s}}, \varphi_{\mathrm{u}}, \varrho_{\mathrm{u}}) \in \mathcal{M}_0\ ;\ \varphi_{\mathrm{u}} + \frac{\omega}{\alpha} \log r\, \varrho_{\mathrm{u}}^{-1} \in I\ \} \tag{14}$$

Thus the image of $\mathcal{M}_I$ is

$$\Pi_{\mathrm{loc}}(\mathcal{M}_I) = \{(\ \varphi_{\mathrm{u}}, \varphi_{\mathrm{s}}, \varrho_{\mathrm{s}}) \in \Sigma^{\mathrm{u}}\ ;\ \varphi_{\mathrm{u}} \in I\ ,\ \varrho_{\mathrm{s}} \leq \tilde{r} \text{ and } \varphi_{\mathrm{s}} = \tilde{g}(\varphi_{\mathrm{u}}, \varrho_{\mathrm{s}})\}$$

where

$$\tilde{g}(\varphi_{\mathrm{u}}, \varrho_{\mathrm{s}}) := g(\varrho_{\mathrm{s}} \cos(\varphi_{\mathrm{u}} - \frac{\omega}{\alpha} \log r\, \varrho_{\mathrm{s}}^{-1}), \varrho_{\mathrm{s}} \sin(\varphi_{\mathrm{u}} - \frac{\omega}{\alpha} \log r\, \varrho_{\mathrm{s}}^{-1})) - \frac{\omega}{\alpha} \log r\, \varrho_{\mathrm{s}}^{-1}.$$

One can now find $\bar{\varrho} > 0$ such that $\tilde{g}(\varphi_{\mathrm{u}}, \cdot)$ as well as $\frac{\partial \tilde{g}}{\partial \varrho_{\mathrm{s}}}(\varphi_{\mathrm{u}}, \cdot)$ are strictly decreasing on $(0, \bar{\varrho}\,]$ for every $\varphi_{\mathrm{u}} \in I$. This is possible because g is bounded in a neighborhood of $\varrho_{\mathrm{s}} = 0$ together with its derivatives. Using this boundedness and applying the chain rule, one arrives at

$$\frac{\partial \tilde{g}}{\partial \varrho_{\mathrm{s}}}(\varphi_{\mathrm{u}}, \varrho_{\mathrm{s}}) = \frac{\omega}{\alpha \varrho_{\mathrm{s}}} + \mathcal{O}(1) \text{ as } \varrho_{\mathrm{s}} \to 0 \tag{15}$$

uniformly in $\varphi_{\mathrm{u}} \in I$. Therefore, $\tilde{g}(\varphi_{\mathrm{u}}, \cdot)$ decreases from infinity on $(0, \bar{\varrho}\,]$ for all $\varphi_{\mathrm{u}} \in I$.
Recall that a scroll was defined as the diffeomorphic image of a reference scroll. We are now able to construct a diffeomorphism $\Psi : Z \to \tilde{Z}$ between

the cylinders $Z := \{ (\varphi_u, \varphi_s, \varrho_s) \in \Sigma^u \; ; \; \varphi_u \in I, \varrho_s \leq \bar{\varrho} \}$ and

$$\tilde{Z} := \{ (\varphi_u, \varphi_s, \varrho_s) \; ; \; \varphi_u \in I, \varrho_s \leq \exp(\frac{\alpha}{\omega}\tilde{g}(\varphi_u, \varrho_s)) \}.$$

Ψ only affects the ϱ_s-coordinate, i.e. $\Psi(\varphi_u, \varphi_s, \varrho_s) := (\varphi_u, \varphi_s, \tilde{\varrho}_s)$ where

$$\tilde{\varrho}_s := \begin{cases} \exp(\frac{\alpha}{\omega}\tilde{g}(\varphi_u, \varrho_s)) \text{ for } \varrho_s \neq 0 \\ 0 \text{ for } \varrho_s = 0 \end{cases}$$

Ψ is one-to-one due to the monotonicity established for $\varrho_s \in (0, \bar{\varrho}]$. To show differentiability of Ψ and Ψ^{-1} one first has to check that

$$\left|\frac{\partial \tilde{g}}{\partial \varrho_s}\right| \text{ and } \left|\frac{\partial \tilde{g}}{\partial \varrho_s}\right|^{-1}$$

are bounded. This can be done easily using the explicit expression for Ψ. Differentiation with respect to the angles φ_s and φ_u causes no trouble since

$$\frac{\partial \tilde{g}}{\partial \varphi_u} = \mathcal{O}(\varrho_s^2) \text{as} \, \varrho_s \to 0.$$

Ψ maps $\Pi_{\text{loc}}(\mathcal{M}_I) \cap Z$ onto

$$\{ (\varphi_u, \varphi_s, \varrho_s) \in \tilde{Z} \; ; \; \varphi_u \in I, \varrho_s = e^{-\varphi_s \alpha/\omega} \}$$

and a affine mapping of $\tilde{Z}$ stretching the interval I onto $[0,1]$ transforms it into the reference scroll $[0,1] \times S_{\alpha/\omega}$.
This proves that $\Pi_{\text{loc}}(\mathcal{M}_I)$ is a logarithmic scroll.

□

An analogous result holds for the local Poincarè-map Π^u_{loc}:

Lemma 15 *For any closed interval $I \subset W^u_{\text{loc}}(0) \cap \Sigma^u$ there is a subset of $Fix(R) \cap \Sigma^0$, such that Π^u_{loc} maps this set onto a logarithmic scroll in Σ^u with basis I.*

We omit the proof of this lemma since it is along the same lines as the proof of the preceding lemma.

6 Infinitely many homoclinic and periodic orbits

The proof of theorem 6 is divided into several parts. After recovering a classical result on 1-periodic orbits we treat the cases of n-homoclinic solutions seperately for n odd and n even.

6.1 A family of 1-periodic orbits

This section contains the result that every reversible homoclinic orbit is surrounded by a family of reversible periodic orbits (see [Dev77], corollary 3.3).

Theorem 16 [1-per, Devaney(1977)] *Assume* **(A1)-(A4)** *and* **(A5')**. *Then there exists a logarithmic spiral $\mathcal{S}$ in $Fix(R)$ with base point $q = \gamma \cap Fix(R)$ such that the associated trajectories of (1) are reversible 1-periodic orbits. The period tends to infinity if the point q is approached along the spiral.*

Proof. We show the existence of a spiral in $Fix(R)$ with base point q consisting of points in $Fix(R) \cap \Pi^{\mathrm{u}}_{1/2}(Fix(R))$. According to lemma 9(iii) the associated orbits are then 1-periodic.
Due to assumption **(A5')**, $Fix(R)$ and $W^{\mathrm{s}}(0)$ intersect transversally in Σ.
To use lemma 15 choose an interval $I \subset W^{\mathrm{u}}_{\mathrm{loc}}(0) \cap \Sigma^{\mathrm{u}}$ containing the point q^{u} in its interior. Then according to lemma 15 a subset of $Fix(R) \cap \Sigma^0$ is mapped to a logarithmic scroll in Σ^{u} by $\Pi^{\mathrm{u}}_{\mathrm{loc}}$.
On the other hand Π^{u} maps a neighborhood of q^{u} in Σ^{u} diffeomorphically to a neighborhood of q in Σ. The part of the scroll lying in the domain of Π^{u} then is mapped into a logarithmic scroll $\mathcal{R}$ in Σ by Π^{u}. The basis of this scroll is a neighborhood of q in W^{u}_q (see figure 5).
Therefore a subset of $Fix(R) \cap \Sigma^0$ (having 0 on its boundary) is mapped onto a logarithmic scroll $\mathcal{R}$ by the Poincaré-map $\Pi^{\mathrm{u}}_{1/2}$. Following lemma 13(iii) the intersection of $\mathcal{R}$ and $Fix(R)$ locally is a spiral $\mathcal{S}$ and the associated orbits are 1-periodic due to lemma 9.

□

This recovers the well-known fact that in reversible systems elementary homoclinic orbits appear as the "limit" of periodic orbits with period tending to infinity. Moreover, the locus of these periodic orbits in $Fix(R)$ is described.

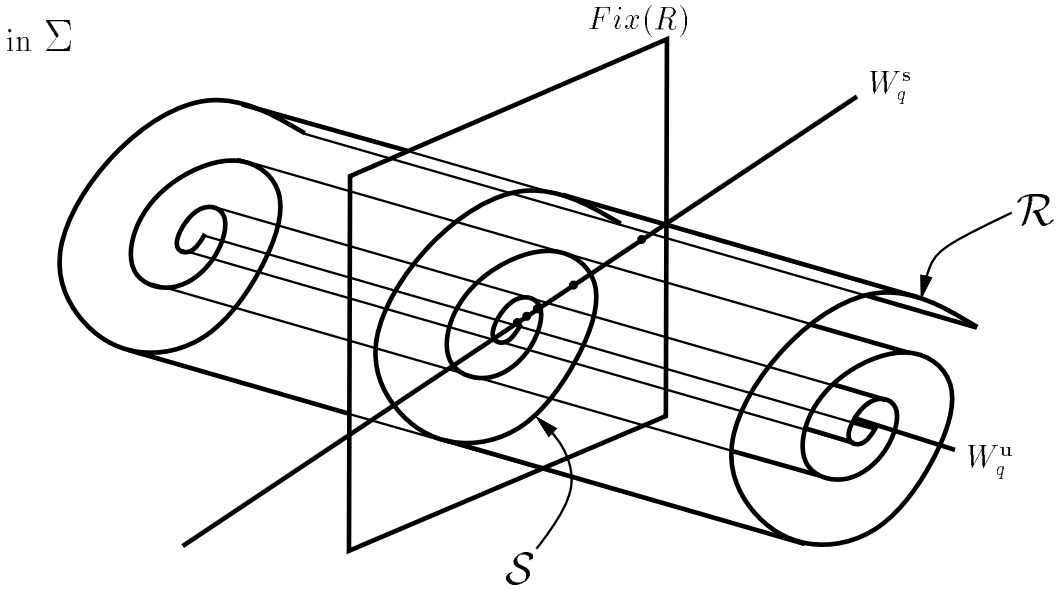

Figure 5: The intersection of $\mathcal{R}$ with $Fix(R)$ in Σ

6.2 (2n+1)-homoclinic and (2n+1)-periodic orbits

The method developped in the previous section allows us to show the existence of n-homoclinic and n-periodic orbits for all $n > 1$. The way we proceed is as follows: A small part of the plane $Fix(R)$ is mapped by an iterate Π^n of the Poincaré-map or by $\Pi^n \circ \Pi^{\mathrm{u}}_{1/2}$ onto a surface that intersects the manifold W^{s}_q transversally. Then a part of this surface will become a logarithmic scroll after one excursion along γ. This logarithmic scroll intersects $Fix(R)$ in a spiral (with the intersection points belonging to periodic orbits) and it has on the other hand a non-empty intersection with W^{s}_q (with intersections belonging to homoclinic orbits). In figure 5 those points of intersection associated with 3-homoclinic orbits are shown. For the proof we essentially apply our lemmata 9 and 10 which stated that, starting in $Fix(R)$, it suffices to construct "semi"-periodic and homoclinic solutions that become "full" periodic and homoclinic solutions by reversibility (see figure 6).

Theorem 17 [(2n+1)-hom] *Let $q_0 \in Fix(R)$ and U be a neighborhood of q_0 in Fix(R) such that $\Pi^n(U)$ and the curve W^{s}_q intersect transversally in $\Pi^n(q_0)$. Then :*
(i) There exists a logarithmic spiral in U with base point q_0 such that the associated orbits are reversible and $(2n+2)-$periodic.
(ii) There exists a sequence of points $p_1, p_2, \ldots$ in U such that the associated orbits are reversible $(2n+3)$-homoclinic orbits.

Proof. Note that according to lemma 10 the orbit of (1) through q_0 is a $(2n+1)$-homoclinic orbit. Our goal is to show that Π^{n+1} maps some piece of

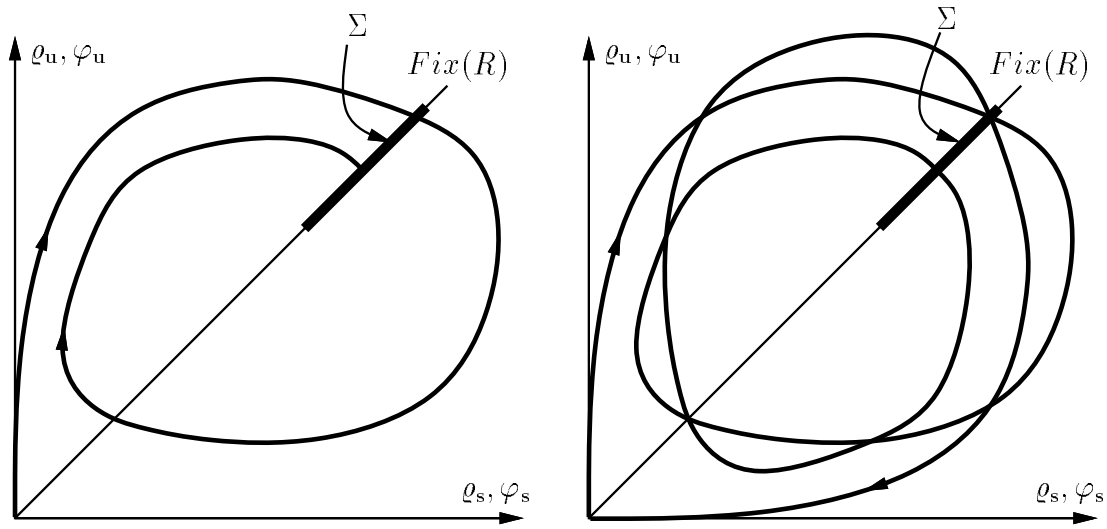

Figure 6: A "semi" 3-homoclinic orbit and a "full" 3-homoclinic orbit

U into a scroll over some part of W_q^u. By lemma 9 every intersection between $\Pi^{n+1}(Fix(R))$ and Fix(R) belongs to a $(2n+2)$-periodic trajectory. Analogously, using lemma 10 intersection points of $\Pi^{n+1}(Fix(R))$ with W_q^s belong to $(2n+3)$-homoclinic orbits.
To find such intersection points, we first choose an interval $I \subset W^u_{loc}(0) \cap \Sigma^u$ that is contained in the domain of Π^u. Since $\Pi^n(U)$ is a two-dimensional C^1-manifold intersecting the curve $W_q^s = (\Pi^s)^{-1}(W^s_{loc}(0) \cap \Sigma^s)$ transversally, by lemma 14 there is a subset U_I of U, such that the image of U_I under $\Pi_{loc} \circ \Pi^s \circ \Pi^n$ is a logarithmic scoll in Σ^u with basis I. The part of the scroll lying in the domain of Π^u is mapped by Π^u into a scroll $\mathcal{R}_I$ in Σ with basis $\Pi^u(I) \subseteq W_q^u$. The plane $Fix(R)$ and the basis of the scroll $\mathcal{R}_I$ intersect transversally in q. By lemma 13(iii) their intersection $\mathcal{R}_I \cap Fix(R)$ is locally a spiral in $Fix(R)$ with base point q. This spiral is contained in $Fix(R) \cap \Pi^{n+1}(Fix(R))$. Hence the associated orbits are $(2n+2)$-periodic ($\rightsquigarrow$ (i)).
According to lemma 13(ii) the intersection $\mathcal{R}_I \cap W_q^s$ consists of a sequence $p_1, p_2, ... \to q$ of points lying in $\Pi^{n+1}(Fix(R)) \cap W_q^s$. Thus, these points lie on $(2n+3)$-homoclinic orbits and (ii) is proved.
By lemma 13(ii) it is clear, that there is an i_0, such that for $i \geq i_0$ the intersection of $\Pi^{n+1}(U)$ and W_q^s in p_i will be transversal.

□

Theorem 16 and theorem 17 together imply immediately:

Corollary 18 ((2n+1)-hom) *Assume* **(A1)-(A5)**. *Then for each* $n \geq 1$ *there exist (countably) infinitely many reversible* $(2n+1)$*-homoclinic orbits and each of this homoclinic orbits is accompanied by a one-parameter-family*

of reversible $(2n+1)$-periodic orbits.

The proof consists of a simple induction. It is only important to notice that the transversality condition **(A5)** on the primary homoclinic orbit γ ensures that infinitely many of the homoclinic orbits found in each step can be considered as new primary homoclinic orbits.

Remark 19 *Theorem 17(ii) seems somewhat surprising at first as one would not expect 4-periodic solutions accumulating to a 3-homoclinic orbit. One should think of those 4-periodic solutions as (3+1)-periodic: Each of those orbits follows alternately a 3-homoclinic orbit and the 1-homoclinic orbit γ. The notation (3+1)-periodic, (5+1)-periodic, etc. in figure 7 is to be understood in this sense.*

6.3 $2n$-homoclinic and $2n$-periodic orbits

To prove the existence of $2n$-homoclinic orbits the second part of lemma 10 will be applied. We proceed in two steps showing the existence of 2-homoclinic orbits first and proving the existence of the other homoclinic solutions by an induction argument.

Theorem 20 (2-hom) *Assume* **(A1)-(A5)**.
Then there is a sequence $p_1, p_2, \ldots \to 0$ in Σ^0 such that the associated trajectories are reversible 2-homoclinic orbits and for $i \geq i_0$ the intersection of $W^{\mathrm{s}}(0)$ and $W^{\mathrm{u}}(0)$ in p_i is transversal.

Proof. The proof runs along the same lines as the proof of theorem 17. A subset of $Fix(R) \cap \Sigma^0$ is mapped by $\Pi^{\mathrm{u}}_{1/2}$ to a logarithmic scroll in Σ over a part of W^{u}_q. The C^1-curve W^{s}_q intersects this scroll in infinitely many points $q_1, q_2, \ldots$. Again, there is an i_0 such that for $i \geq i_0$ the intersection of the scroll with W^{s}_q in q_i is transverse.
The points $p_i := (\Pi^{\mathrm{u}}_{1/2})^{-1}(q_i)$ possess the properties claimed in the theorem.

□

Remark 21 *Again, replacing* **(A5)** *by* **(A5')** *yields infinitely many 2-homoclinic orbits which may be degenerate.*

The preceding theorem enables us now to show inductively that there are also homoclinic orbits following γ an even number of times. This theorem

completes the proof of theorem 6.

Theorem 22 [2n-hom & 2n-per] *For each $n \geq 1$ there are infinitely many reversible $2n$-homoclinic orbits and each of them is accompanied by a family of reversible $2n$-periodic orbits.*
The intersections of such a family of periodic orbits with $\Sigma^0 \cap Fix(R)$ form a logarithmic spiral in $Fix(R)$, with a base point that belongs to one of the homoclinic orbits.

Proof. Each of the 2-homoclinic orbits whose existence was obtained in theorem with $i \geq i_0$ can be considered as a new 1-homoclinic orbit. Using theorem 16 one gets (with respect to the primary homoclinic orbit γ) a family of reversible 2-periodic trajectories.
Corollary 18 yields then infinitely many $2(2n+1)$-homoclinic and $2(2n+1)$-periodic orbits and theorem 20 shows the existence of infinitely many 4-homoclinic orbits.
One can proceed by induction and conclude from the existence of 2^k-homoclinic trajectories that there exist 2^k-periodic, $2^k(2n+1)$-homoclinic, $2^k(2n+1)$-periodic and 2^{k+1}-homoclinic orbits.

□

Thereby we have proved theorem 6: From the existence of a single reversible homoclinic orbit we immediately get the existence of infinitely many n-homoclinic and n-periodic orbits for all $n \geq 2$.

7 Discussion

Without rigorous proof, we want to indicate first, how our branches of 3-periodic and (3+1)-periodic solutions are related to the branches of subharmonic periodic orbits found by Vanderbauwhede [Van90]. He shows that branches of n-periodic orbits bifurcate from the branch of 1-periodic solutions if a Floquet multiplier crosses a n-th root of unity along this branch. There is a distinction between the branching of $2n$-periodic solutions and of $(2n+1)$-period solutions. While in the latter case there is one branch of bifurcating solutions, in the former case there are two half-branches. For brevity, we restrict our considerations here to the case of 3- and 4-periodic solutions to demonstrate the geometrical difference. There are two ways of getting reversible 4-periodic solutions:
a) as intersections of $\Pi^2(Fix(R))$ with $Fix(R)$ in Σ or
b) as intersections of $(\Pi^{\mathrm{s}}_{1/2} \circ \Pi \circ \Pi^{\mathrm{u}}_{1/2})(Fix(R))$ with $Fix(R)$ in Σ^0.
The solutions one gets in either case are not the same since the 4-periodic

orbits of case a) have their symmetric points in Σ while the solutions from case b) have both symmetric points in Σ^0.
Case a) corresponds to the 4-periodic solutions accumulating onto 3-homoclinic orbits, while case b) covers those 4-periodic orbits that accumulate onto 4-homoclinic orbits. Nevertheless, one can check that sufficiently close to q or 0 all branches of 4-periodic solutions cross the primary branch of 1-periodic solutions. This can be shown by taking into account the domains of the different Poincaré-maps in the analysis of the previous section.
Hence, the branch of 1-periodic solutions divides the branch of 4-periodic solutions in two half-branches that are mapped onto each other by Π^2 in case a) or by $\Pi^s_{1/2} \circ \Pi \circ \Pi^u_{1/2}$ in case b). Figure 7 indicates how these branches lie in $Fix(R)$.
The situation is different for 3-periodic solutions: Here the two possibilities
a) intersection of $(\Pi^s_{1/2} \circ \Pi)(Fix(R))$ with $Fix(R)$ in Σ and
b) intersection of $(Pi \circ \Pi^u_{1/2})(Fix(R))$ with $Fix(R)$ in Σ^0
yield the same branch of 3-periodic solutions. These solutions have one symmetric point in Σ and the other one in Σ^0. The map $\Pi^u_{1/2} \circ \Pi$ maps one branch onto the other.

The theorems proved in section 6 show that there is an abundance of homoclinic and periodic orbits intersecting the plane $Fix(R)$ near 0 and near q. Figure 7 tries to give an impression of the way how those various homoclinic and periodic orbits lie in $Fix(R)$. Due to self-similarity each of the spirals looks approximately like the whole picture.

Unfortunately, there are still only a few examples where the existence of a reversible homoclinic orbit has been proved. In the work of Iooss and Kirchgässner [IK92] on solitary water waves in a cylinder, a partial differential equation is reduced to a four-dimensional reversible system using normal form theory. Homoclinic orbits of this equation correspond to solitary waves in the original problem. Especially, the n-homoclinic orbits are solitary waves with n humps. The same fourth-order equation also arises in a model describing buckling of an elastic strut, which was examined by Amick and Toland [AT92]. Champneys and Toland [CT93] proved the existence of a reversible homoclinic orbit and also its transversality. Numerical calculations performed on this equation by Buffoni, Champneys and Toland [CT93,BCT94] do confirm the results on n-homoclinic solutions and show that the homoclinic solutions can be continued over a large parameter regime until they coalesce in pairs [BCT94]. For both cases, recent work of Sandstede [San,San96] adresses the important issue of stability of the n-pulse solutions with respect to the partial differential equation.
Peletier and Troy in [PT95]. have considered the extended Fisher-Kolmogorov (EFK) equation. This equation possesses a pair of non-reversible, but symmetric equilibria (with respect to R). The existence of heteroclinic orbits connecting these two equilibria is proved for certain values of a parameter. Our results

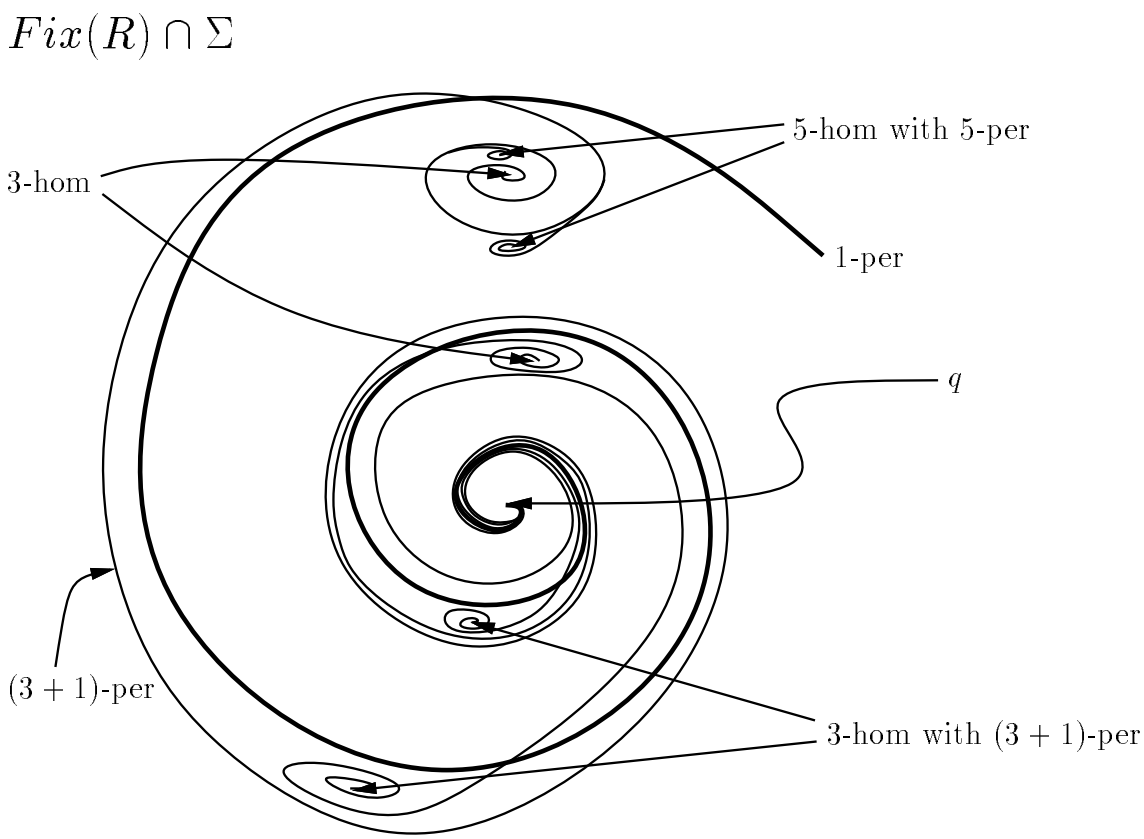

Figure 7: The location of homoclinic and periodic orbits in Σ

should easily carry over to their case, if only a transversality condition such as **(A5)** holds. One should then be able to prove the existence of heteroclinic and homoclinic orbits (kinks) and periodic orbits.

Acknowledgement

I would like to thank B. Fiedler for proposing the subject of reversible homoclinic orbits and for many suggestions and encouragement. Thanks are also due to B. Sandstede and A. Champneys for helpful discussions and to G. Iooss for pointing out the relevance of condition **(A5')**.

References

[AT92] C. J. Amick and J. F. Toland. Homoclinic orbits in the dynamic phase

space analogy of an elastic strut. *Europ. J. Appl. Math.*, **3**:97–114, 1992.

[BCT94] B. Buffoni, A. R. Champneys, and J. F. Toland. Bifurcation and coalescence of a plethora of homoclinic orbits for a Hamiltonian system. Preprint, 1994.

[Bel73] G. R. Belitskii. Functional equations and conjugacy of local diffeomorphisms of a finite smoothness class. *Funct. Anal. Appl.*, **7**:268–277, 1973.

[Cha94] A. R. Champneys. Subsidiary homoclinic orbits to a saddle-focus for reversible systems. *Int. J. Bif. Chaos*, **4**:1447–1482, 1994.

[CT93] A. R. Champneys and J. F. Toland. Bifurcation of a plethora of multi-modal homoclinic orbits for autonomous Hamiltonian systems. *Nonlinearity*, **6**:665–772, 1993.

[Dev77] R. L. Devaney. Blue sky catastrophes in reversible and hamiltonian systems. *Ind. Univ. Math. J.*, **26**:247–263, 1977.

[Har82] P. Hartman. *Ordinary Differential Equations*. Birkhäuser Verlag, Boston, 1982.

[Här93] J. Härterich. Kaskaden homokliner Orbits in reversiblen dynamischen Systemen. Diplomarbeit, Universität Stuttgart, 1993.

[IK92] G. Iooss and K. Kirchgässner. Water waves for small surface tension: an approach via normal form. *Proc. Royal Soc. Edinburgh*, **122 A**:267–299, 1992.

[PT95] L. A. Peletier and W. C. Troy. Spatial patterns described by the extended Fisher-Kolmogorov (EFK) equation: kinks. *Diff. Int. Eq.*, **8**:1279–1304, 1995.

[San] B. Sandstede. Stability of multiple-pulse solutions. Preprint, to appear in Trans. Amer. Math. Soc.

[San95] B. Sandstede. Center manifolds for homoclinic solutions. Preprint, WIAS Berlin, 1995.

[San96] B. Sandstede. Instability of localised buckling modesin a one-dimensional strut model. Preprint, to appear in Phil. Trans. R. Soc. London A, 1996.

[Shi67] L. P. Shil'nikov. The existence of a denumerable set of periodic motions in four-dimensional space in an extended neighborhood of a saddle-focus. *Sov. Math. Dokl.*, **8**:54–57, 1967.

[Van90] A. Vanderbauwhede. Subharmonic branching in reversible systems. *SIAM J. Math. Anal.*, **21**:954–979, 1990.

[VF92] A. Vanderbauwhede and B. Fiedler. Homoclinic period blow-up in reversible and conservative systems. *Z. angew. Math. Phys.*, **43**:292–318, 1992.